J. Fluid Mech. (1996), *vol.* 323, *pp.* 267–283

Solidification of pressure-driven flow in a finite rigid channel with application to volcanic eruptions

By JOHN R. LISTER AND PAUL J. DELLAR

Institute of Theoretical Geophysics, Department of Applied Mathematics and Theoretical Physics, University of Cambridge, Silver Street, Cambridge CB3 9EW, UK

(Received 1 March 1996 and in revised form 8 May 1996)

Competition between conductive cooling and advective heating occurs whenever hot fluid invades a cold environment. Here the solidification of hot viscous flow driven by a fixed pressure drop through an initially planar or cylindrical channel embedded in a cold rigid solid is analysed. At early times, or far from the channel entrance, the flow starts to solidify and block the channel, thus reducing the flow rate. Close to the channel entrance, and at later times, the supply of new hot fluid starts to melt back the initial chill. Eventually, either solidification or meltback becomes dominant throughout the channel, and flow either ceases or continues until the source is exhausted. The evolution of the dimensionless system, which is characterized by the initial Péclet number Pe, the Stefan number S and the dimensionless solidification temperature Θ, is calculated numerically and by a variety of asymptotic schemes. The results show the importance of variations along the channel and caution against models based on a single 'representative' width. The critical Péclet number Pe_c, which marks the boundary between eventual solidification and eventual meltback, is determined for a wide range of parameters and found to be much larger for cylindrical channels than for planar channels, owing to the slower rate of decay of the heat flux into the solid in a cylindrical geometry. For a planar channel Pe_c is given by the simple algebraic result $Pe_c \sim 0.46[\Theta^2/(1-\Theta)(S+2/\pi)]^3$ when $(1-\Theta)^{-1} \gg S \gg 1$, but in general it requires numerical solution. Similar analyses, in which there is a spatially varying and time-dependent interaction between the rates of solidification and flow, have a range of applications to geological and industrial processes.

1. Introduction

In many industrial processes, such as injection moulding and continuous casting, hot fluid is forced to flow between cold boundaries against which solidification of the fluid can occur. Similarly, during volcanic eruptions hot magma must traverse a conduit from the magmatic source to the surface through much colder crustal rock, and some solidification of the magma is bound to occur. In both of these cases solidification will constrict the flow and it is natural to ask how the flow will evolve and whether the flow might become completely blocked. Since the rate of solidification depends in part on the advective heat transport by the fluid and the fluid velocity depends in part on the amount by which solidification constricts the flow, the thermal evolution and the fluid-dynamical response are intimately

coupled and investigation of such problems reveals interesting nonlinear and time-dependent behaviour. While complex interactions between solidification and flow occur in a variety of settings and parameter regimes, we shall consider here a simple fundamental problem, which arose as a model for the evolution of basaltic fissure eruptions.

Solidification in magmatic conduits has often been treated as decoupled from the flow, and the heat transfer and solidification rates calculated as if the magma were at rest, thus completely neglecting any effects of advection (e.g. Fedotov 1978; Wilson & Head 1981; Turcotte & Schubert 1982). However, calculations for both rigid (Delaney & Pollard 1982; Bruce & Huppert 1989, 1990) and deformable (Lister 1994*a*,*b*) conduits show that advective heat transfer plays a crucial role in determining variations in the rate of solidification along the conduit and the consequent evolution of the flow. Both Delaney & Pollard (1982) and Bruce & Huppert (1989, 1990), referred to hereafter as DP and BH, considered flow along a fissure leading from a source of magma at constant overpressure to eruption at the surface. The chief physical assumptions made in the derivation of their models were that the fissure was initially approximately planar and of constant width, that it was formed and filled with hot magma on a much shorter timescale than the subsequent solidification, that the rapid increase in viscosity from the magmatic liquidus to the solidus can be represented by a simple solidification temperature below which the magma ceases to flow, and that the flow itself is laminar and the conduit walls rigid. Justification for these assumptions and further details of the physical modelling and geological observations can be found in the original papers. We will not, therefore, rehearse the geological motivation further here.

The geologically motivated studies may be compared with a series of studies (e.g. Ockendon & Ockendon 1977; Richardson 1983, 1986) of channel flow with temperature-dependent viscosity, which were motivated by applications to polymer processing. While there is clearly some rheological similarity between a sharp increase in viscosity and solidification, calculations of channel flow with temperature-dependent viscosity differ thermally by omitting the latent heat involved in a phase change and by including the possibility of thermal runaway due to viscous dissipation. For the case that viscous dissipation is negligible, as in geological flows, the studies with temperature-dependent viscosity have largely concentrated on steady entry flows rather than the time-dependent problem, though there have been some recent investigations of a thermoviscous fingering instability analogous to the Saffman–Taylor mechanism (Helfrich 1995; Wylie & Lister 1995; Morris 1996).

We commence with the basic fluid-mechanical problem of solidification of two-dimensional laminar flow in an initially planar channel of finite length embedded in a cold rigid solid, and then also consider the analogous problem for axisymmetric flow in an initially cylindrical channel. Before calculating numerical solutions, DP and BH made a number of further mathematical simplifications to this basic problem, which are discussed in §2. In §3 we calculate solutions to the full system of equations in order to assess the accuracy of the previous results and extend them to a much larger parameter range. We are also able to derive asymptotic solutions in the limits of large Stefan number and large undercooling in §4, which can be used to define a simple approximate criterion for the flow to block completely. The axisymmetric case is analysed in §5, and the results and possible extensions are discussed in §6. Finally, we note that similarity solutions in the various asymptotic regions of the early-time behaviour, including the near-source effects of advection, melting and variable width, can be obtained analytically as described in the Appendix.

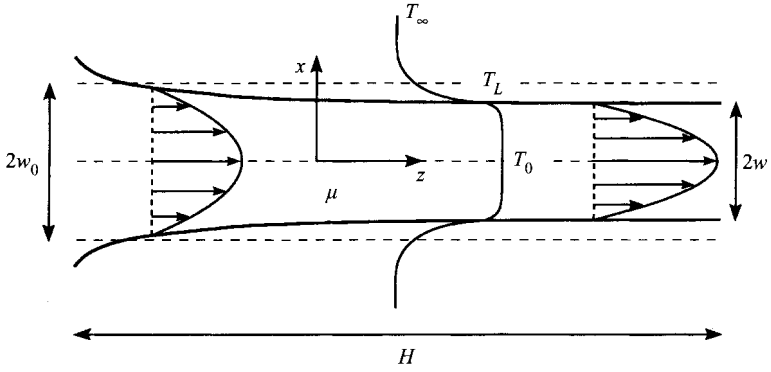

FIGURE 1. A planar channel of width $2w(z,t)$ and length H is embedded in a solid with far-field temperature T_∞. Fluid of viscosity μ supplied at temperature T_0 is driven along the channel by a constant pressure difference ΔP. The width of the channel evolves owing to solidification and melting at temperature T_L.

2. Flow in a planar channel

2.1. *The governing equations*

Consider a planar channel extending from $z = 0$ to $z = H$ with rigid boundaries initially at $x = \pm w_0$ (figure 1). We suppose that at $t = 0$ the channel $|x| < w_0$ is filled with fluid at temperature T_0 and that the region $|x| > w_0$ is occupied by solid at temperature T_∞. For $t > 0$ the fluid is driven along the channel by a constant pressure difference ΔP, while fluid at temperature T_0 is supplied to the channel at $z = 0$ to replace that expelled at $z = H$. We suppose, for simplicity, that the fluid and the solid are indistinguishable except by phase and have a common solidification temperature T_L, where $T_\infty < T_L < T_0$. As a result of solidification and melting, the phase boundary defining the walls of the channel evolves to $x = \pm w(z,t)$.

We define a dimensionless temperature by

$$\theta = \frac{T - T_\infty}{T_0 - T_\infty} \tag{2.1}$$

and non-dimensionalize the remaining variables with respect to the scales

$$\hat{z} = H, \qquad \hat{x} = w_0, \qquad \hat{u}_z = \frac{\Delta P w_0^2}{\mu H}, \qquad \hat{u}_x = \frac{\hat{u}_z w_0}{H}, \qquad \hat{t} = \frac{w_0^2}{\kappa}, \tag{2.2}$$

where μ is the dynamic viscosity of the fluid and κ is the thermal diffusivity.

The parameter regime of geological interest is $(\hat{u}_z w_0/\nu)(w_0/H) \ll 1$, where ν is the kinematic viscosity, and $\hat{u}_z w_0/\kappa \gg 1$, corresponding to long thin channels and fluid of large viscosity and low thermal conductivity. Provided also that the Reynolds number $\hat{u}_z w_0/\nu$ is no more than about 10^3 (so that the flow is laminar and not turbulent), it then follows that the fluid velocity can be calculated by lubrication theory and that alongstream conduction can be neglected in comparison with cross-stream conduction. In accord with previous analyses (e.g. DP; BH) and for simplicity, we also neglect the effects of heating by viscous dissipation and cooling by adiabatic decompression.

By the usual analysis of lubrication flow, the velocity along the channel is given by $u_z = \frac{3}{4}Q(w^2 - x^2)/w^3$, where the volume flux Q is related to the local pressure gradient by $Q = -\frac{2}{3}w^3(\partial p/\partial z)$. The small cross-stream velocity u_x can be calculated from u_z

by local continuity and the volume flux Q can be calculated from the conditions that $\partial Q/\partial z = 0$ (even with solidification) and that the total pressure drop is unity with the scalings (2.2). Thus the fluid velocity is given by

$$\boldsymbol{u} = \frac{3Q}{4}\frac{w^2 - x^2}{w^3}\left(\frac{xw_z}{w}, 1\right) \qquad (|x| \leqslant w) \tag{2.3}$$

where

$$Q = \frac{2}{3}\left(\int_0^1 w^{-3}\mathrm{d}z\right)^{-1} \tag{2.4}$$

and w_z denotes $\partial w/\partial z$.

Since alongstream conduction is negligible, the temperature of the fluid evolves according to

$$\theta_t + Pe\,\boldsymbol{u}\cdot\nabla\theta = \theta_{xx}, \tag{2.5}$$

where the subscripts denote partial derivatives and Pe is a modified Péclet number, which describes the relative importance of advection and cross-stream conduction and is defined by

$$Pe = \frac{\Delta P\, w_0^4}{\kappa\mu H^2}. \tag{2.6}$$

The temperature in the solid obeys the standard diffusion equation, $\theta_t = \theta_{xx}$. The boundary conditions at the walls of the channel, the entrance to the channel and $t = 0$ are

$$Sw_t = [\theta_x]^+_-, \tag{2.7}$$

$$\theta(w, z, t) = \Theta, \tag{2.8}$$

$$\theta(x, 0, t) = 1 \qquad (|x| < w), \tag{2.9}$$

$$\theta(x, z, 0) = 1 \qquad (|x| < w), \tag{2.10}$$

$$\theta(x, z, 0) = 0 \qquad (|x| > w), \tag{2.11}$$

where $[\theta_x]^+_- \equiv \theta_x(w_+) - \theta_x(w_-)$ denotes the jump in the conductive flux across $x = w$ due to the release of latent heat; the Stefan number and dimensionless solidification temperature are defined by

$$S = \frac{L}{C_p(T_0 - T_\infty)} \quad \text{and} \quad \Theta = \frac{T_L - T_\infty}{T_0 - T_\infty}, \tag{2.12}$$

where L is the latent heat and C_p is the specific heat capacity.

Equations (2.3)–(2.5) and (2.7)–(2.11) comprise the basic problem to be solved, which depends only on the three parameters Pe, S and Θ. Some qualitative understanding of the pattern of solidification and melting can be obtained by consideration of the solution at early times when the temperature gradients are confined to thin thermal boundary layers at $x = \pm 1$. Far from $z = 0$ the effects of advection are not felt at early times, the balance in (2.5) is between the first and third terms ($\theta_t \sim \theta_{xx}$) and the solution is given by that for a semi-infinite body of fluid placed in contact with a semi-infinite solid; the width of the boundary layer increases like $t^{1/2}$ and if $\Theta > \frac{1}{2}$ the fluid solidifies at a rate proportional to $t^{-1/2}$. Close to $z = 0$, however, the continual supply of hot fluid at $z = 0$ produces a quasi-steady boundary layer in the fluid in which there is a balance between alongstream advection and cross-stream diffusion, and the large heat flux across this boundary layer causes melting of the

channel walls. On the assumption that the shear rate close to the wall is $O(1)$, a balance between the second and third terms ($Pe(w-x)\theta_z \sim \theta_{xx}$) of (2.5) gives a boundary layer of width $O(z/Pe)^{1/3}$. Comparison of the boundary-layer thicknesses in the two regions ($t^{1/2} \sim (z/Pe)^{1/3}$) shows that the transition between near-source melting and far-from-source solidification occurs when $z = O(Pe\ t^{3/2})$. It may also be noted that very close to $z = 0$ (actually $z \ll Pe\ t^3$) the heat flux from the fluid and the consequent rate of melting are so large that w is no longer $O(1)$ and the boundary-layer scalings have to be modified. Detailed analytic solutions for the boundary-layer structure in the three regions $z \ll Pe\ t^3$, $Pe\ t^3 \ll z \ll Pe\ t^{3/2}$ and $Pe\ t^{3/2} \ll z$, and for the matching between these solutions, are given in the Appendix.

These qualitative arguments suggest a competition between two processes. On the one hand, as the temperature gradient in the solid broadens diffusively and solidification rates far from the source decrease, the region in which advective supply of heat produces melting extends down the channel. On the other hand, constriction of the channel due to solidification in the downstream region decreases the flow rate Q and the strength of advection. As discussed by BH, there are thus two possibilities for the eventual behaviour depending on which of these processes becomes dominant: if Pe is sufficiently large then the region of melting extends along the whole channel before it can be blocked and the channel subsequently widens and the flow rate increases until the source is exhausted; if Pe is smaller than a critical value then the channel becomes blocked at the downstream end and flow ceases. The critical value $Pe_c(S, \Theta)$ is determined in the following sections.

2.2. *Discussion of previous approximate solutions*

Both DP and BH made a number of simplifying approximations to the basic problem in order to reduce the computational task. DP approximated the temperature in the solid by part of an error-function profile, chosen to satisfy (2.7) and (2.8) in which, moreover, S was set to zero. The temperature in the fluid was approximated by a two-term boundary-layer expansion of quasi-steady solutions to (2.5) in powers of $(z/Pe)^{1/3}$ (Newmann 1969). The velocity field itself was approximated by assuming that $\partial p/\partial z$ was constant, so $Q \propto w^3$ locally, rather than imposing the integral constraint (2.4).

BH patched the short-time solution for $z \gg Pe\ t^{3/2}$ to a subsequent evolution in which the full diffusion equation was solved in the solid but the heat flux from the fluid was approximated in a number of ways. Since the channel solidifies most rapidly at $z = 1$, it was assumed that (2.4) could be approximated by $Q = \frac{2}{3}w(1)^3$ and the shear rate along the walls by the uniform value $w(1)$. This shear rate was then substituted into the steady solution (Leveque 1928) for a thermal boundary layer in uniform shear flow past a plane wall without solidification in order to calculate the heat flux and then use (2.7) to obtain $\mathrm{d}w(1)/\mathrm{d}t$.

While many of these approximations have some justification, particularly the use of a quasi-steady boundary-layer approach for large Pe before the channel becomes significantly constricted, it is desirable to solve the full system of equations in order to check their accuracy.

3. Numerical results

In order to solve (2.6) numerically, it is convenient to map the fluid region onto a fixed rectangular domain (see e.g. Crank 1984). Accordingly, we define $\bar{x} = x/w$ so

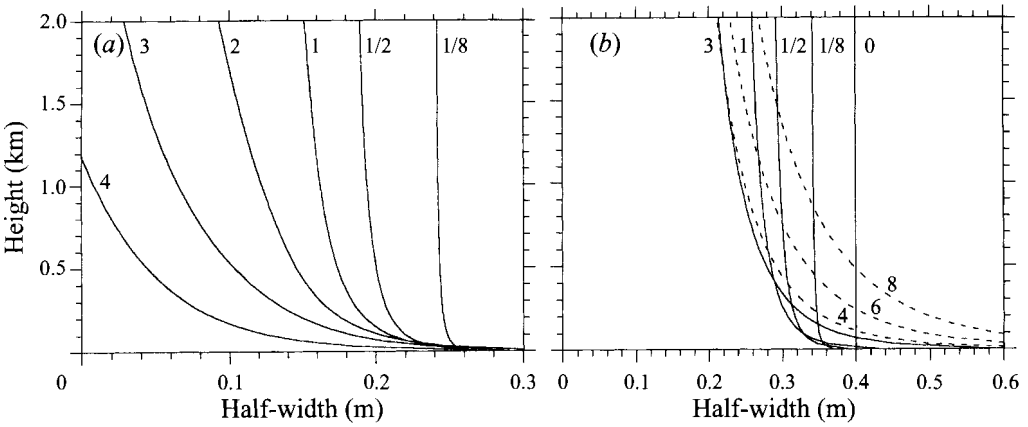

FIGURE 2. The evolution of the half-width $w(z,t)$ for $S = 1$ and $\Theta = 0.9$. The results have been made dimensional by using the illustrative geological parameters $\Delta P/H = 2000\,\mathrm{Pa\,m^{-1}}$, $\mu = 100\,\mathrm{Pa\,s}$, $H = 2\,\mathrm{km}$ and $\kappa = 10^{-6}\,\mathrm{m^2 s^{-1}}$ from BH and the marked times are in days. (*a*) A channel of initial width $2w_0 = 60$ cm, corresponding to $Pe = 81$, is blocked by solidification; (*b*) meltback is sufficiently strong in an 80 cm channel, corresponding to $Pe = 256$, to keep the flow going until the supply is exhausted.

that (2.5) and (2.7) become

$$\theta_t + \frac{3QPe}{4}\frac{1-\bar{x}^2}{w}\theta_z - \frac{w_t}{w}\bar{x}\theta_{\bar{x}} = \frac{\theta_{\bar{x}\bar{x}}}{w^2}, \qquad (|\bar{x}| < 1), \tag{3.1}$$

$$Sww_t = [\theta_{\bar{x}}]^+_-. \tag{3.2}$$

The z-derivative in (3.1) was represented using a flux-conservative Lax–Wendroff scheme and the $\bar{x}$-derivatives using a Crank–Nicolson discretization. A time-dependent grid expanding away from $\bar{x} = 1$ was used to resolve the early growth of the thermal boundary layers near the wall. The integral in (2.4) was evaluated from a piece-wise linear representation of w. Nonlinear coefficients were evaluated at a half-timestep in order to obtain a final scheme that was second order in both time and space. The accuracy of the calculations was tested by conservation of energy, by comparison with asymptotic solutions such as those described in the following sections, and by grid-doubling.

In figure 2 we show the evolution of the half-width of a planar channel for $S = 1$ and $\Theta = 0.9$, for which the critical Péclet number $Pe_c \approx 131$. The variation of the width with z, even at early times, shows that the supply of heat by advection slows the rate of solidification near the entrance. For $Pe = 81$ (figure 2*a*) this supply of heat is never sufficient to produce melting over more than 4% of the channel length and the flow soon solidifies. For $Pe = 256$ (figure 2*b*) the stronger flow is sufficient to keep the channel open and eventually produce melting along the entire channel.

In figure 3 we illustrate solutions on either side of the critical Péclet number, which show an initially similar conductive evolution followed by a dramatic divergence due to blocking or dominance of advection. The differences between the minimum width $w(1)$, a mean width $(\overline{w^{-3}})^{-1/3}$ based on flow rate (see (2.4)) and a mean width $(\overline{w^{-1}})^{-1}$ based on heat flux (see (4.4)) suggests that simplified models that neglect the variation with z and use only a single representative width are unlikely to be accurate.

In figure 4 we show the critical Péclet number as a function of S and Θ. For a given Péclet number, the tendency to block increases with the rate of solidification

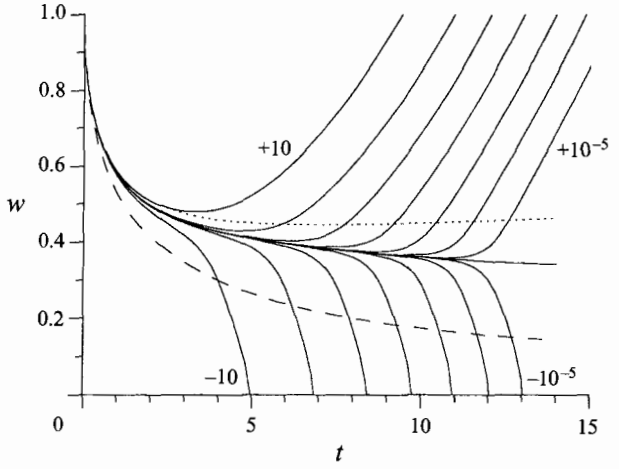

FIGURE 3. The evolution of the minimum width $w(1)$ (dashed), and the 'mean' widths $(\overline{w^{-1}})^{-1}$ (dotted) and $(\overline{w^{-3}})^{-1/3}$ for $S = 1$ and $\Theta = 0.9$ and $Pe = Pe_c \approx 131$. Also shown (solid) is the evolution of $(\overline{w^{-3}})^{-1/3}$ for $Pe = Pe_c \pm 10^i$, $i = -5, -4, \ldots, 1$.

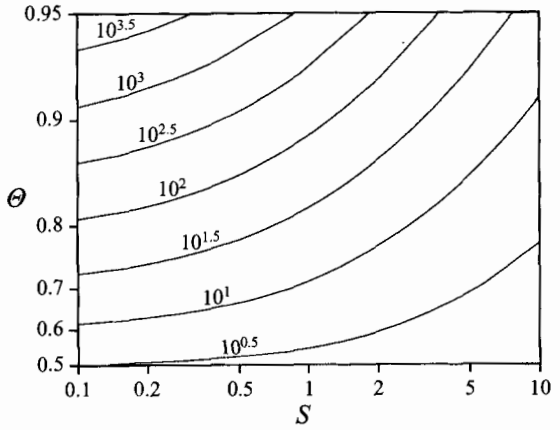

FIGURE 4. Contours of the critical Péclet number for a two-dimensional channel as a function of S and Θ.

and so Pe_c increases as $\Theta \to 1$ and as S decreases. The computational cost increases with Pe_c owing to the increasing disparity between the small timesteps allowable by the Courant condition and the long diffusive timescale of solidification.

4. Asymptotic solutions

4.1. *The limit* $S \to \infty$

As $S \to \infty$, the solidification rate w_t is $O(S^{-1})$ and can be neglected in (3.1). We then rescale the along-channel coordinate by defining

$$\zeta(z) = \frac{2}{3QPe} \int_0^z \frac{\mathrm{d}z}{w} = \frac{1}{Pe} \int_0^1 \frac{\mathrm{d}z}{w^3} \int_0^z \frac{\mathrm{d}z}{w} \tag{4.1}$$

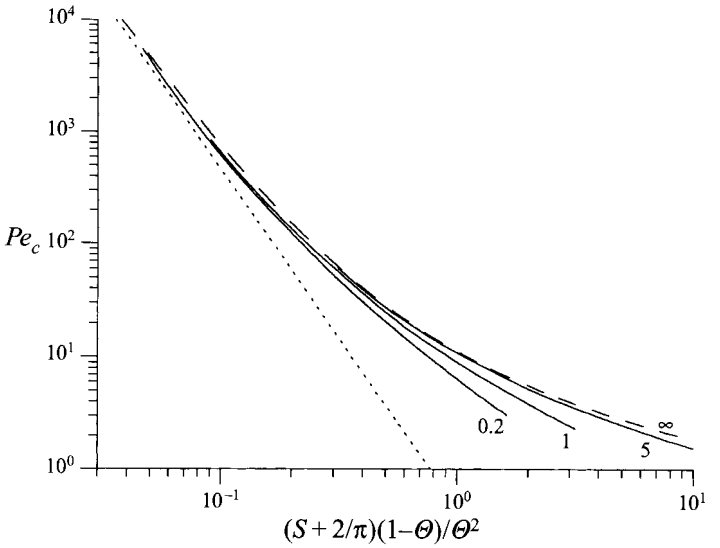

FIGURE 5. Comparison of the critical Péclet number as found from the large-S asymptotic system, (4.1) and (4.4), (dashed curve) with that from the full solution for $S = 0.2$, 1 and 5. The asymptotic results give good agreement even at moderate values of S. The dotted line is the combined large-S, large-Pe result, (4.8).

so that (3.1) becomes

$$\tfrac{1}{2}(1-\bar{x}^2)\theta_\zeta = \theta_{\bar{x}\bar{x}} \tag{4.2}$$

subject to $\theta(1,\zeta) = \Theta$ and $\theta(\bar{x},0) = 1$. This is a standard thermal-entry problem (Graetz 1885) for which solutions can be obtained by eigenfunction expansion or numerically. We write $\theta_{\bar{x}}(1_-,z) = (1-\Theta)f(\zeta)$, where f is found by solving the Graetz problem.

Neglect of w_t also allows the temperature and heat flux in the solid to be written as

$$\theta(x,z) = \Theta\,\mathrm{erfc}\big[(x-w)/2t^{1/2}\big] \quad \text{and} \quad \theta_x(w_+,z) = -\Theta/(\pi t)^{1/2}. \tag{4.3}$$

We now substitute the expressions for the heat flux into (2.7), rescale the time by defining $\tau = \Theta^2 t/S^2$ and obtain

$$w_\tau = \frac{(1-\Theta)S}{\Theta^2}\frac{f(\zeta)}{w} - \frac{1}{(\pi\tau)^{1/2}}. \tag{4.4}$$

It is consistent with the asymptotic limit $S \to \infty$ to replace S in (4.4) by $S + c$, where c is any given constant, and heuristically we choose $c = 2/\pi$, both by analogy with an expansion of the coefficient λ in the half-space solidification problem (see Carslaw & Jaeger 1959, p. 288; or (A2d) in the Appendix) and because it gives a better fit of the asymptotic behaviour to results for finite values of S. With this replacement the asymptotic system (4.1) and (4.4) depends only on Pe and the combination parameter $(1-\Theta)(S+2/\pi)/\Theta^2$.

The equations were solved numerically by discretizing w with z and then using a Runge–Kutta method to solve (4.4) as a set of ordinary differential equations linked by (4.1). The solutions show the same behaviour as those described in §3. In figure 5 we show the critical Péclet number and compare it with the results from the full calculation plotted against $(1-\Theta)(S+2/\pi)/\Theta^2$. It may be seen that there is

remarkably good agreement with the large-S asymptotic at quite small values of S, particularly at large values of Pe.

4.2. *The limit* $Pe \to \infty$

As $Pe \to \infty$ the temperature gradients in the fluid are confined to thin thermal boundary layers of width $O(Pe^{-1/3})$ against the walls. If $1-\Theta$ is $O(1)$ then the large heat flux across these boundary layers will rapidly cause melting along the length of the channel and the flow will subsequently increase monotonically. If the channel is to be significantly constricted or even blocked by solidification it follows that $1-\Theta \ll 1$ and hence $w_t\theta_x \ll \theta_{xx}$. Thus the fluid temperature can again be calculated from solution of the quasi-steady equations (4.1) and (4.2). Moreover, $\zeta \ll 1$ since $Pe \gg 1$ and hence the asymptotic form of the boundary heat flux from the Leveque solution,

$$f(\zeta) \sim \frac{(3/\zeta)^{1/3}}{\Gamma\left(\frac{1}{3}\right)} \approx 0.5383\zeta^{-1/3}, \tag{4.5}$$

can be used.

The rate of solidification can, however, no longer be neglected in the calculation of the temperature in the solid. We define a new coordinate by $x' = x - w$ so that

$$\theta_t - w_t\theta_{x'} = \theta_{x'x'} \qquad (x' > 0). \tag{4.6}$$

Since $1-\Theta \ll 1$, we can set $\theta = 1$ rather than Θ on $x' = 0$. The value of w_t in (4.6) is calculated from

$$Sw_t = (1-\Theta)\frac{0.5383}{w\zeta^{1/3}} + \theta_{x'}(0_+, z). \tag{4.7}$$

The form of (4.1), (4.6) and (4.7) shows that the evolution in this limit depends only on S and the combination parameter $Pe(1-\Theta)^3$.

Numerical solution in this limit requires much less computation than the full problem since, though (4.6) still requires solution of a diffusion problem at each z, the timestep is not constrained by the Courant condition for the alongstream advection in the fluid. Results for the critical Péclet number scaled by $(1-\Theta)^3$ are shown in figure 6. Convergence to the asymptotic limit is quite slow in this case.

4.3. *Comparison of results*

Comparison of the asymptotic results for $S \to \infty$ and $Pe \to \infty$ shows that in the joint limit $S \to \infty$, $S(1-\Theta) \to 0$ the critical Péclet number has the form

$$Pe_c \sim 0.46\left(\frac{\Theta^2}{(1-\Theta)(S+2/\pi)}\right)^3, \tag{4.8}$$

where the multiplying constant was evaluated numerically. Heuristic arguments leading to the same dimensional dependence on parameters, but a less accurate determination of the constant, were given by Bruce (1989) and Petford, Lister & Kerr (1994).

In figure 7 we compare the critical Péclet number, as found from the full system of equations (2.3)–(2.11), with the values determined from the asymptotic schemes for $S \to \infty$ and $Pe \to \infty$, and the approximate scheme described by BH. The large-S asymptotic scheme is the most effective approximation over the range of values shown, though the large-Pe asymptotic scheme provides a small improvement for $S < 1$ and $Pe > 1000$.

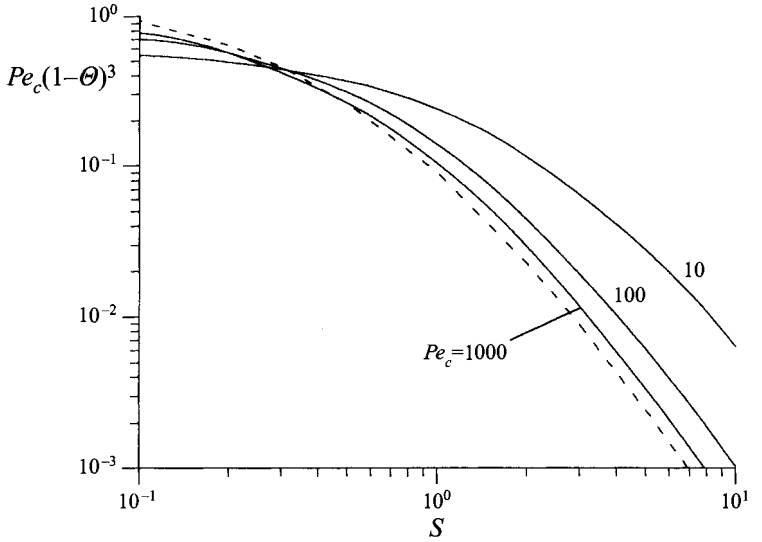

FIGURE 6. Comparison of the critical Péclet number as found from the large-Pe asymptotic system, (4.1), (4.6) and (4.7) (dashed), with that from the full solution (solid). The axes are chosen to exhibit the collapse of $(1-\Theta)^3 Pe_c$ against S as $Pe \to \infty$.

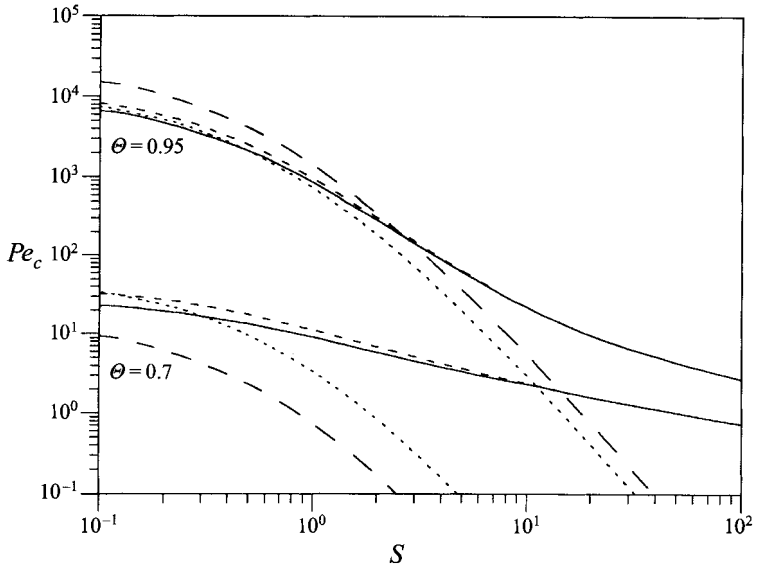

FIGURE 7. Comparison of the critical Péclet number as found from the full equations (solid), the large-S asymptotic system (short dashed), the large-Pe asymptotic system (dotted), and the approximation described by BH (long dashed).

5. Flow in an axisymmetric channel

We describe briefly the adaptations to the foregoing analysis of a planar channel that are required to calculate the evolution of solidification and flow in an initially cylindrical channel of radius w_0. Maintaining the same non-dimensionalization as in (2.1), the velocity along an axisymmetric channel of radius $w(z,t)$ is given by $u_z = -\frac{1}{4}(w^2 - r^2)(\partial p/\partial z)$, and the volume flux Q is related to the local pressure

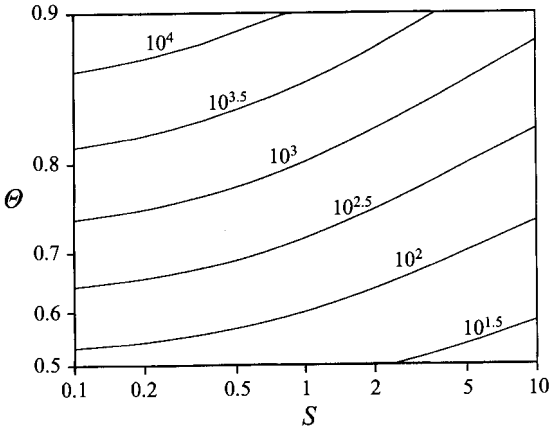

FIGURE 8. Contours of the critical Péclet number for an axisymmetric channel as a function of S and Θ. The values of Pe_c are much larger than the corresponding values for a planar channel (figure 4).

gradient by $Q = -\frac{1}{8}\pi w^4(\partial p/\partial z)$. Thus

$$\boldsymbol{u} = \frac{2Q}{\pi}\frac{w^2 - r^2}{w^4}\left(\frac{rw_z}{w}, 1\right) \qquad (r \leqslant w) \tag{5.1}$$

where

$$Q = \frac{\pi}{8}\left(\int_0^1 w^{-4}\mathrm{d}z\right)^{-1}. \tag{5.2}$$

The temperature of the fluid evolves according to

$$\theta_t + Pe\,\boldsymbol{u}\cdot\nabla\theta = \theta_{rr} + \theta_r/r, \tag{5.3}$$

where Pe is given by (2.6). The temperature in the solid now obeys the axisymmetric diffusion equation, $\theta_t = \theta_{rr} + \theta_r/r$, but the boundary conditions are directly analogous to (2.7)–(2.11).

We define $\bar{r} = r/w$ so that (5.3) becomes

$$\theta_t + \frac{2QPe}{\pi}\frac{1-\bar{r}^2}{w^2}\theta_z - \frac{w_t}{w}\bar{r}\theta_{\bar{r}} = \frac{\theta_{\bar{r}\bar{r}} + \theta_{\bar{r}}/\bar{r}}{w^2} \qquad (\bar{r} < 1). \tag{5.4}$$

Comparison of (5.2) and (5.4) with the planar equivalents, (2.4) and (3.1), shows that the effects of the axisymmetric geometry are apparent in the stronger dependence of flow rate on w and, more significantly, in the form of the conductive cooling. The heat flux outside a hot cylinder eventually decays only like $1/\ln t$, in comparison with the faster $t^{-1/2}$ decay next to a hot planar wall. Since the evolution of a solidifying channel typically takes many diffusion timescales owing to the buffering effect of the latent heat, the heat flux outside an axisymmetric channel enters this slowly decaying regime and, in consequence, it is harder for the advected heat flux to keep an axisymmetric channel open for long enough for meltback to occur. Thus the critical Péclet numbers for an axisymmetric geometry (figures 8 and 9) tend to be much larger than the corresponding values for a planar geometry (figure 4).

5.1. *Asymptotic models*

Some asymptotic progress can be made along the lines of §4, though the analysis is less successful in an axisymmetric geometry. By neglecting w_t and rescaling the

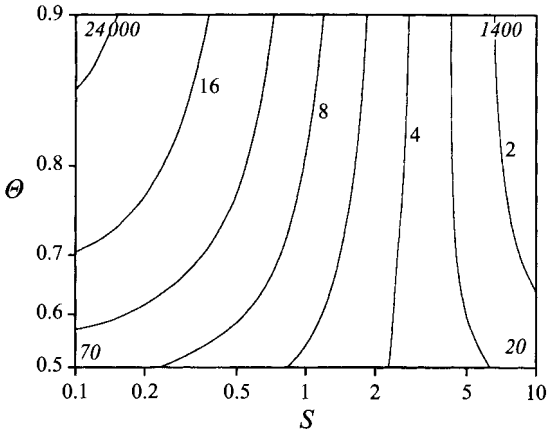

FIGURE 9. Contours of $(1-\Theta)^3 Pe_c$ for an axisymmetric channel as a function of S and Θ. The scaling with $(1-\Theta)^3$ removes most of the Θ dependence, as for a planar channel, but the dependence on S is much weaker than the S^3 of (4.8). The italic numbers in the corners are the unscaled values of Pe_c.

along-channel coordinate by

$$\zeta(z) = \frac{\pi z}{4QPe} = \frac{z}{2Pe}\int_0^1 \frac{\mathrm{d}z}{w^4}, \tag{5.5}$$

we reduce (5.4) to

$$\tfrac{1}{2}(1-\bar{r}^2)\theta_\zeta = \theta_{\bar{r}\bar{r}} + \theta_{\bar{r}}/r \tag{5.6}$$

subject to $\theta(1,\zeta) = \Theta$ and $\theta(\bar{r},0) = 1$. Thus $\theta_{\bar{r}}(1_-,z) = (1-\Theta)F(\zeta)$, where F is found by solving the standard cylindrical thermal-entry problem. The heat flux from a cylinder of fixed radius maintained at fixed temperature is given by Carslaw & Jaeger (1959, p. 336, equation 8), but, unlike the corresponding flux in (4.3), is not a simple power law and depends on the radius of the cylinder. The large-S asymptotic evolution equation is thus written

$$Sww_t = (1-\Theta)F(\zeta) - \Theta G(t/w^2), \tag{5.7}$$

where $G(t)$ is the flux from a unit cylinder maintained at unit temperature. While Θ and S cannot be grouped as in (4.4), equations (5.5) and (5.7) can still be solved economically as a coupled set of ordinary differential equations for discretized values $w(z_i)$.

Asymptotic analysis in the limit $Pe \to \infty$ leads again to (4.7), but now with $\theta_{x'}$ given by solving the axisymmetric diffusion equation outside a cylinder of variable radius $w(t)$ and fixed temperature Θ. Though the leading-order expansion of $F(\zeta)$ is the same as that of $f(\zeta)$ in (4.5), the corrections are larger in an axisymmetric geometry and more accurate results are obtained if these are retained. The largest corrections to the Leveque boundary-layer solution are due to the curvature of the Poiseuille flow and of the boundary rather than to the neglect of w_t. We therefore recommend a composite approximation for $S \to \infty$ or $Pe \to \infty$ that is given by (5.5) and

$$Sw_t = \frac{(1-\Theta)F(\zeta)}{w} + \theta_r(w_+,z), \tag{5.8a}$$

$$\theta_t = \theta_{rr} + \theta_r/r, \qquad \theta(w,z) = \Theta\,. \tag{5.8b,c}$$

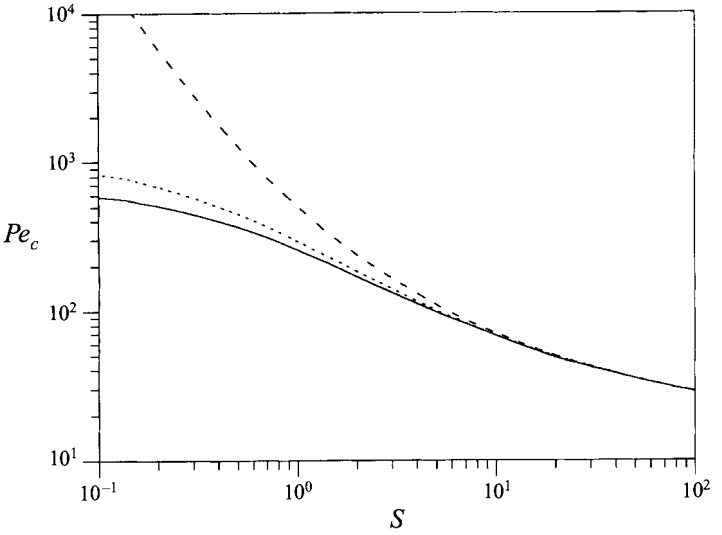

FIGURE 10. Comparison of the critical Péclet number for an axisymmetric channel as found from the full equations (solid), the large-S asymptotic (5.7) (dashed) and the composite asymptotic (5.8) (dotted). All curves are for $\Theta = 0.7$.

This gives the critical Péclet number to within 20% in the region $S > 1$ and $\Theta > 0.6$.

Results from the two asymptotic approximations (5.7) and (5.8) are compared with the full solution in figure 10.

6. Discussion

We have analysed the evolution by solidification and melting of a hot flow through a channel embedded in a cold solid. There is a competition between the tendency of conductive cooling to narrow the channel by solidification and the tendency of advective supply of heat by the flow to widen the channel by melting back first the initial chill and then the walls of the channel. The analytic solution for the short-time behaviour shows that solidification is initially dominant owing to the large thermal gradients, but, as these decrease, melting extends over a growing region near the source of the flow. However, the flow rate also decreases owing to continued solidification at the downstream end of the channel, thereby reducing the advective supply of heat. The balance of this competition between solidification and melting thus varies with time and along the channel, but is eventually resolved decisively one way or another: either solidification becomes dominant throughout the channel and the flow is blocked, or melting becomes dominant and flow continues until the source is exhausted. Blocking is favoured by long, narrow channels, low driving pressures, large viscosities, small latent heats, large undercoolings and small initial superheats.

We have calculated the critical Péclet number that determines whether a flow ultimately blocks or melts back both by numerical solution of the full equations and by various asymptotic approximations. These results extend previous approximate solutions (DP; BH) to a much wider range of Stefan numbers and solidification temperatures, and to axisymmetric geometry. It is notable that critical Péclet numbers in an axisymmetric geometry are much larger than those in planar geometry owing to the slower $O(1/\ln t)$, rather than $O(t^{-1/2})$, decay of the heat flux into the solid.

Interestingly, pipe-like volcanic conduits are observed to be typically much wider than planar conduits.

It is also worth commenting on a suggestion by BH that two-dimensional evolution in a planar geometry would be unstable to flow localization in the third (transverse) direction. The suggested mechanism – that locally increased flow increases the heat supply, widens the channel, reduces the flow resistance and further increases the flow – should also apply to pressure-driven flow of fluid with temperature-dependent viscosity in a cooled planar channel. However, recent studies of the latter problem (Helfrich 1995; Wylie & Lister 1995; Morris 1996) have shown that flow localization only occurs when the flow is relatively slow so that the thermal entry length is reached and the viscosity variations lie across the flow (as in the Saffman–Taylor instability), and not when the flow is relatively fast so that temperature and viscosity variations lie in boundary layers roughly parallel to the flow. If it can be argued that a solidified layer is like a very viscous boundary layer then instability would not be expected here, though it should be noted that the problems are not exactly analogous and this question requires further study before it is resolved.

The various solutions described in §§3–5 form the basis of a hierarchy of numerical methods, which can be ordered by accuracy and computational expense. Solution of the full set of equations is computationally expensive, owing to the need to take timesteps based on an advective timescale in order to satisfy the Courant condition, while following the evolution on the much longer conductive timescale. By neglecting $\partial w/\partial t$, the temperature in the fluid can be assumed to be quasi-steady and the corresponding heat flux into the channel wall taken from a simple rescaling of the standard thermal entry-length problem. This approximation, which is used in (4.7) and (5.8), reduces the problem to calculation of heat transfer in the solid and allows the timestep to be significantly increased to a conductive timescale. The next level of approximation, which is used in the large-Stefan-number approximations (4.4) and (5.7), is also to neglect $\partial w/\partial t$ in the solid and then to take the corresponding heat flux from solutions for a fixed planar or cylindrical boundary maintained at constant temperature. This reduces the calculation to a set of coupled ordinary differential equations for the widths at a discretized set of locations along the channel. Finally, we note the simple algebraic expression (4.8) for the critical Pećlet number that results from the combination of these approximations in the planar case.

While we have analysed here the simple fundamental problem of flow through a channel embedded in a uniform, infinite solid of the same material as the fluid, there is a wide range of extensions to this problem with applications to geological and industrial processes. For the geological case, desirable extensions include allowing elastic deformation of the channel wall and considering variations $w_0(z)$ and $T_\infty(z)$ in the initial channel width and far-field temperature (Lister 1995). Industrial applications would typically allow the chill but not the channel walls to melt and either apply fixed-temperature boundary conditions at the channel wall or consider a wall of finite thickness. It is envisaged that some of the asymptotic and numerical ideas developed here can readily be adapted to these problems, in each of which the phenomena of interest arise from the spatial and temporal interactions between solidification and flow.

Appendix. A boundary-layer solution for early times

At early times the temperature gradients are confined to thin thermal boundary layers near $x = \pm w$. Except for a small region near $z = 0$, where there is very rapid

melting, w is still close to unity and hence $Q \sim \frac{2}{3}$. We define $X = w - x$ and $Z = z/Pe$ and can thus write (2.5) for $t \ll 1$ as

$$\theta_t + w^{-1}X\theta_Z + w^{-1}w_t\theta_X \sim w^{-2}\theta_{XX} \qquad (X > 0). \tag{A 1}$$

For $Z \gg t^3$, $w \sim 1$ and the solution to (A1) can be obtained by use of the similarity variables $\xi = X/t^{1/2}$ and $\zeta = Z/t^{3/2}$ (Lister 1994*b*, (3.8) ff.). In $Z \gg t^{3/2}$ alongstream advection is negligible and the similarity solution $\vartheta(\xi, \zeta)$ asymptotes to

$$\vartheta \sim \frac{\Theta \operatorname{erfc}\{-(\xi/2 + \lambda)\}}{\operatorname{erfc}(-\lambda)} \qquad (\xi \leqslant 0), \tag{A 2a}$$

$$\vartheta \sim 1 - \frac{(1-\Theta)\operatorname{erfc}\{\xi/2 + \lambda\}}{\operatorname{erfc}\lambda} \qquad (\xi \geqslant 0), \tag{A 2b}$$

$$w_t \sim -\lambda t^{-1/2}, \tag{A 2c}$$

where

$$S\pi^{1/2}\lambda e^{\lambda^2} = \frac{\Theta}{\operatorname{erfc}(-\lambda)} - \frac{(1-\Theta)}{\operatorname{erfc}\lambda}. \tag{A2d}$$

(The difference between the asymptotic solution $\lambda \sim (2\Theta - 1)/\pi^{1/2}(S + 2/\pi)$ as $\lambda \to 0$ of (A2*d*) and the approximation $\lambda \sim (2\Theta - 1)/\pi^{1/2}S$ obtained by neglecting w_t in (A1) motivates the replacement of S by $S + 2/\pi$ in equation (4.4).) In $t^3 \ll Z \ll t^{3/2}$ the temperature is quasi-steady and the similarity solution asymptotes to

$$\vartheta(\eta) = 1 - \frac{(1-\Theta)\displaystyle\int_\eta^\infty \exp(\Lambda\eta - \eta^3/9)\,\mathrm{d}\eta}{\displaystyle\int_0^\infty \exp(\Lambda\eta - \eta^3/9)\,\mathrm{d}\eta} \qquad (\eta \geqslant 0), \tag{A3a}$$

$$\vartheta(\eta) = \Theta\, e^{\Lambda\eta} \qquad (\eta \leqslant 0), \tag{A3b}$$

$$w_t = \Lambda Z^{-1/3}, \tag{A3c}$$

where

$$\Lambda \int_0^\infty \exp(\Lambda\eta - \eta^3/9)\,\mathrm{d}\eta = \frac{1-\Theta}{S+\Theta} \tag{A3d}$$

and $\eta = X/Z^{1/3} = \xi/\zeta^{1/3}$.

From (A3*c*) it can be seen that the approximation $w \sim 1$ in (A1) is only valid when $Z \gg t^3$, as stated earlier. When $Z = O(t^3)$ we seek a quasi-steady solution to (A1) by putting

$$\zeta = \frac{Z}{t^3}, \qquad w = W(\zeta), \qquad \eta = \frac{X}{tY(\zeta)}, \tag{A 4}$$

where W and Y must be solved for as functions of the similarity variable ζ. Substitution into (A1) and (2.7) gives

$$\vartheta_{\eta\eta} - S^{-1}[\vartheta_\eta]_-^+\vartheta_\eta = -\eta^2\vartheta_\eta(WY^2Y_\zeta) \qquad (\eta > 0) \tag{A5a}$$

$$S(3\zeta W W_\zeta Y) = [\vartheta_\eta]_-^+. \tag{A5b}$$

It follows that the solution for ϑ is given by (A3*a*,*b*) provided that

$$WY^2Y_\zeta = \tfrac{1}{3} \quad \text{and} \quad 3\zeta W W_\zeta Y = \Lambda. \tag{A 6}$$

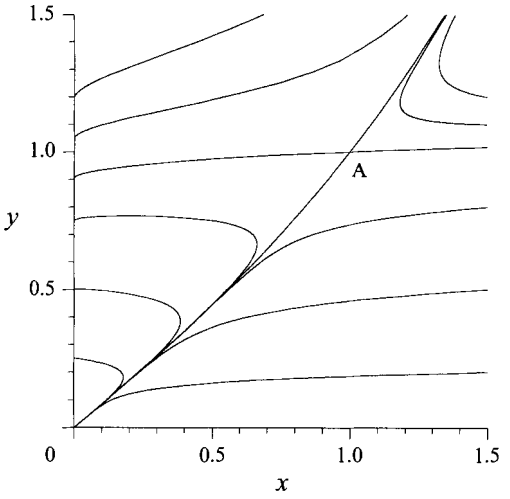

FIGURE 11. The (x, y) phase plane for (A8). The near-origin similarity solution to (A1) in $Z \ll t^{3/2}$ is obtained from the trajectory that joins the singular point A = (1, 1) to the origin.

To solve (A6) we let $u = (15/\Lambda)^3\zeta$ and $F = (15Y/\Lambda)^3$ so that (A6) becomes

$$W = 1/F_u \quad \text{and} \quad uF_{uu}F^{1/3} = 5(F_u)^3. \tag{A 7}$$

We then let $v = \frac{6}{5}\ln(u/6)$, $x = Fe^{-v}$ and $y = F_v e^{-v}$ in order to obtain the autonomous system

$$x_v = y - x \quad \text{and} \quad y_v = \tfrac{1}{6}y(y^2x^{-1/3} - 1). \tag{A 8}$$

By consideration of the (x, y) phase plane (figure 11), it is straightforward to show that the desired solution is given by the trajectory that connects the singular point at (1,1) to the singular point at (0,0). As $v \to \infty$, we find that $x \sim 6e^{-v/6}$, $y \sim 5e^{-v/6}$, $F \sim u$, $Y \sim \zeta^{1/3}$ and $W \sim 1$, which corresponds to the solution in $t^3 \ll Z \ll t^{3/2}$. As $v \to -\infty$, we find that $x \sim y \sim 1$, $F \sim (u/6)^{6/5}$, $Y \sim (15\zeta^2/36\Lambda)^{1/5}$ and $W \sim (50\Lambda^3/9\zeta)^{1/5}$, which corresponds to the solution in $Z \ll t^3$.

REFERENCES

BRUCE, P. M. 1989 Thermal convection within the Earth's crust. PhD thesis, University of Cambridge.

BRUCE, P. M. & HUPPERT, H. E. 1989 Thermal control of basaltic fissure eruptions. *Nature* **342**, 665–667 (referred to herein as BH).

BRUCE, P. M. & HUPPERT, H. E. 1990 Solidification and melting in dykes by the laminar flow of basaltic magma. In *Magma Transport and Storage* (ed. M.P. Ryan). Wiley (referred to herein as BH).

CARSLAW, H. S. & JAEGER, J. C. 1959 *Conduction of Heat in Solids*. Oxford University Press.

CRANK, J. 1984 *Free and Moving Boundary Problems*. Oxford University Press.

DELANEY, P. T. & POLLARD, D. D. 1982 Solidification of basaltic magma during flow in a dike. *Am. J. Sci.* **282**, 856–885 (referred to herein as DP).

FEDOTOV, S. A. 1978 Ascent of basic magmas in the crust and the mechanism of basaltic fissure eruptions. *Intl Geol. Rev.* **20**, 33–48.

GRAETZ, L. 1885 Über die Wärmeleitungsfähigkeit von Flüssigkeiten. *Ann. Phys. Chem.* **25**, 337–357.

HELFRICH, K. R. 1995 Thermo-viscous fingering of flow in a thin gap: application to magma emplacement. *J. Fluid Mech.* **305**, 219–238.

LEVEQUE, M. A. 1928 Les lois de la transmission de chaleur par convection. *Ann. Mines Mem.* **13**, 201–299.

LISTER, J. R. 1994*a* The solidification of buoyancy-driven flow in a flexible-walled channel. Part 1. Constant-volume release. *J. Fluid Mech.* **272**, 21–44.

LISTER, J. R. 1994*b* The solidification of buoyancy-driven flow in a flexible-walled channel. Part 2. Continual release. *J. Fluid Mech.* **272**, 45–65.

LISTER, J. R. 1995 Fluid-mechanical models of the interaction between solidification and flow in dykes. In *Physics and Chemistry of Dykes*, (ed. G. Baer & A. Heimann), pp. 115–124. Balkema.

MORRIS, S. J. S. 1996 Stability of thermoviscous Hele-Shaw flow. *J. Fluid Mech.* **308**, 111–128.

NEWMANN, J. 1969 Extension of the Leveque solution. *J. Heat Transfer* **91**, 177–178.

OCKENDON, H. & OCKENDON, J. R. 1977 Variable-viscosity flows in heated and cooled channels. *J. Fluid Mech.* **83**, 177–190.

PETFORD, N., LISTER, J. R. & KERR, R. C. 1994 The ascent of felsic magmas in dykes. *Lithos* **32**, 161–168.

RICHARDSON, S. M. 1983 Injection moulding of thermoplastics: Freezing during mould filling. *Rheol. Acta* **22**, 223–236.

RICHARDSON, S. M. 1986 Injection moulding of thermoplastics: Freezing of variable viscosity fluids. II. Developing flows with very low heat generation. *Rheol. Acta* **25**, 308–318.

TURCOTTE, D. L. & SCHUBERT, G. 1982 *Geodynamics*. John Wiley

WILSON, L. & HEAD, J. W. 1981 Ascent and eruption of basaltic magma on the Earth and Moon. *J. Geophys. Res.* **86**. 2971–3001.

WYLIE, J. J. & LISTER, J. R. 1995 The effect of temperature-dependent viscosity on flow in a cooled channel with application to basaltic fissure eruptions. *J. Fluid Mech.* **305**, 239–261.